Phase control of group-velocity-based biexciton coherence in a multiple quantum well nanostructure

Seyyed Hossein Asadpour† and H. Rahimpour Soleimani

Department of Physics, University of Guilan, Rasht, Iran

(Received 8 January 2014; revised manuscript received 5 March 2014; published online 10 August 2014)

A double cascade-type four-level multiple-quantum-well-based exciton–biexciton transitions are proposed. The study is carried out on a 4.8-nm ZnSe single-quantum well which is embedded into ZnMgSSe cladding layers and pseudomorphically grown by molecular beam epitaxy on a (0 0 1) GaAs substrate. It is displayed that the exciton spin relaxation and relative phases between applied fields can influence the transient and steady-state behaviors of absorption, dispersion, and group velocity of two weak probe and signal fields. Also, transient behaviors of electron population of different levels are discussed. It is found that the probe or signal amplification occurs in the absence of population inversion.

Keywords: exciton-spin relaxation, biexciton coherence, relative phase between applied fields

PACS: 42.50.−p, 42.65.−k **DOI:** 10.1088/1674-1056/23/10/104205

1. Introduction

Due to the small effective electron mass, semiconductor quantum wells have advantages of high nonlinear optical coefficients and large electric dipole moments. Also, they have properties similar to atomic vapors such as the discrete levels. This means that semiconductor quantum wells have received significant attention to application in quantum optics. The theory of quantum coherence phenomena in semiconductor quantum dot (QD) was introduced by Chow *et al.*[1] Recently, several interesting phenomena such as electromagnetically induced transparency (EIT),[2–6] lasing without inversion (LWI),[7] four-wave mixing (FWM),[8–11] optical bistability (OB),[12–27] slow light,[2] and many others[28–45] in atomic systems, semiconductors, and solid states medium have been discussed and demonstrated by different research groups. In the EIT medium, the strong coherent laser fields provide the atomic phase coherence that is responsible for transparency of the medium. In fact, EIT is a technique for eliminating the effect of a medium on propagation beam of the electromagnetic radiation. So, in the EIT medium not only the weak probe field will not be absorbed but also a refractive index curve with very steep gradient will appear.[46] EIT is also the mechanism underlying the recent experiments in ultra-slow group velocity of a probe pulse and therefore greatly increases the effective interaction time of the pulse with the medium.[47,48] In LWI, it was found that if atomic coherence and interference between certain atomic states is granted, different absorption processes may interfere destructively, leading to the reduction or even the cancelation of absorption. At the same time, stimulated emission may remain intact, leading to the possibility of gain even if only a small fraction of the population inversion is in the excited state.[49] Note that the implementation of EIT and LWI in semiconductor-based devices is very attractive from view point of applications. One of the most distinguished features in the coherent optical response of a semiconductor arising from Coulomb-correlation effects is the spectral signature of the bound-biexciton state. A signature of this two-photon coherence may also occur in the optical response. Under ultrashort-pulse excitation the coherent dynamics of the optically generated electron–hole pairs is strongly governed by correlation effects induced by the Coulomb interaction among them.[50] With intersubband coherence between different conduction subbands[51–53] and different valance subbands,[54,55] and with intervalence band coherence between the heavy-hole (HH) and light-hole (LH) valance bands,[56–58] EIT processes have also been observed. EIT may lead to great enhancement in nonlinear effect and steep dispersion, as well as to the reduction of group velocity, the storage of optical pulses.[59,60] The coherent control of exciton and exciton–biexciton transitions for wave mixing signal generation in the SQWs was also discussed.[61]

It is also known that the relative phase of the applied laser fields as a method to study quantum coherent control and interference has been widely used in several important processes in atomic, molecular, and solid-state systems.[62–67] But the transient behavior and group velocity of probe and signal fields in a quantum well nanostructure via phase control of biexciton coherence have not been investigated.

In this paper, the effects of relative phase between applied fields and exciton spin relaxation on the transient behaviors of two weak probe and signal fields are discussed. Also it is shown that under the various parametric conditions the group velocities of the probe and signal fields can be controlled.

†Corresponding author. E-mail: S.Hosein.Asadpour@gmail.com

© 2014 Chinese Physical Society and IOP Publishing Ltd

2. Model and equations

The double-cascade four-level system in semiconductor single-quantum well has exploited the usage of excitons spin coherence. The study is carried out on a 4.8-nm ZnSe single-quantum well which is embedded into ZnMgSSe cladding layers and has pseudomorphically grown by molecular beam epitaxy on a (0 0 1) GaAs substrate. As shown schematically in Fig. 1, the ground state $|0\rangle$, one-exciton states $|1\rangle$, $|2\rangle$, and biexciton state $|3\rangle$ resemble a four-level cascade configuration.[68–70] In the present system, two pulsed probe fields (P,S) with angular frequencies ω_p, ω_S, one-half Rabi frequencies Ω_p, Ω_S, and two continues wave coherent couple fields (c_1, c_2) with angular frequency ω_{c1}, ω_{c2}, one-half Rabi frequency $\Omega_{c1,c2}$, complete the respective excitation. Under the rotating wave approximation and electric dipole approximation, the time evolution of the system, expressed using the density operator ρ, is governed by the Liouville equation which leads to the following equations for the density matrix elements:

$$
\begin{aligned}
\dot{\rho}_{11} &= \mathrm{i}\Omega_p(\rho_{01}-\rho_{10})+\mathrm{i}\Omega_{c1}(\rho_{31}-\rho_{13})+\gamma_a\rho_{22}\\
&\quad-(\gamma_b+\gamma_4)\rho_{11}+\gamma_2\rho_{33},\\
\dot{\rho}_{22} &= \mathrm{i}\Omega_s(\rho_{02}-\rho_{20})+\mathrm{i}\Omega_{c2}(\mathrm{e}^{\mathrm{i}\phi}\rho_{32}-\mathrm{e}^{-\mathrm{i}\phi}\rho_{23})+\gamma_1\rho_{33}\\
&\quad-(\gamma_3+\gamma_a)\rho_{22}+\gamma_b\rho_{11},\\
\dot{\rho}_{33} &= +\mathrm{i}\Omega_{c2}(\mathrm{e}^{-\mathrm{i}\phi}\rho_{23}-\mathrm{e}^{\mathrm{i}\phi}\rho_{32})+\mathrm{i}\Omega_{c1}(\rho_{13}-\rho_{31})\\
&\quad-(\gamma_1+\gamma_2)\rho_{33},\\
\dot{\rho}_{10} &= -(1/2(\gamma_4+\gamma_b+\gamma_{10}^{\mathrm{dph}})-\mathrm{i}\Delta_1)\rho_{10}+\mathrm{i}\Omega_p(\rho_{00}-\rho_{11})\\
&\quad+\mathrm{i}\Omega_{c1}\rho_{30}-\mathrm{i}\Omega_s\rho_{12},\\
\dot{\rho}_{20} &= -(1/2(\gamma_3+\gamma_a+\gamma_{20}^{\mathrm{dph}})-\mathrm{i}\Delta_2)\rho_{20}+\mathrm{i}\Omega_s(\rho_{00}-\rho_{22})\\
&\quad+\mathrm{i}\Omega_{c2}\mathrm{e}^{\mathrm{i}\phi}\rho_{30}-\mathrm{i}\Omega_p\rho_{21},\\
\dot{\rho}_{30} &= -(1/2(\gamma_1+\gamma_2+\gamma_{30}^{\mathrm{dph}})-\mathrm{i}\Delta_3)\rho_{30}+\mathrm{i}\Omega_{c1}\rho_{10}\\
&\quad+\mathrm{i}\Omega_{c2}\mathrm{e}^{-\mathrm{i}\phi}\rho_{20}-\mathrm{i}\Omega_s\rho_{32}-\mathrm{i}\Omega_p\rho_{31},\\
\dot{\rho}_{32} &= -(1/2(\gamma_1+\gamma_2+\gamma_3+\gamma_{32}^{\mathrm{dph}})-\mathrm{i}(\Delta_3-\Delta_1))\rho_{32}\\
&\quad-\mathrm{i}\Omega_{c2}\mathrm{e}^{\mathrm{i}\phi}(\rho_{33}-\rho_{22})-\mathrm{i}\Omega_{c1}\rho_{21}+\mathrm{i}\Omega_s\rho_{03},\\
\dot{\rho}_{21} &= -(1/2(\gamma_b+\gamma_3+\gamma_4+\gamma_a+\gamma_{21}^{\mathrm{dph}})-\mathrm{i}(\Delta_1-\Delta_2))\rho_{21}\\
&\quad-\mathrm{i}\Omega_p\rho_{20}-\mathrm{i}\Omega_{c1}\rho_{23}+\mathrm{i}\Omega_{c2}\mathrm{e}^{\mathrm{i}\phi}\rho_{31}+\mathrm{i}\Omega_s\rho_{01},\\
\dot{\rho}_{31} &= -(1/2(\gamma_1+\gamma_2+\gamma_4+\gamma_b+\gamma_{31}^{\mathrm{dph}})-\mathrm{i}(\Delta_1-\Delta_3))\rho_{31}\\
&\quad+\mathrm{i}\Omega_p\rho_{03}+\mathrm{i}\Omega_{c1}(\rho_{33}-\rho_{11})-\mathrm{i}\Omega_{c2}\mathrm{e}^{\mathrm{i}\phi}\rho_{12}, \qquad (1)
\end{aligned}
$$

where

$$
\begin{aligned}
&\rho_{ij}=\rho_{ij}^{*},\ \ \Delta_j=\omega_{p(s)}-(\omega_j-\omega_0)\ (J=1,2),\\
&\Delta_3=\omega_{p(s)}+\omega_{cj}-(\omega_3-\omega_0),
\end{aligned}
$$

the latter, $\gamma_{ij}^{\mathrm{dph}}$ is the dephasing broadening linewidth, which may originate from electron–electron scattering, electron–phonon scattering as well as inhomogeneous broadening due to scattering on interface roughness. Generally, $\gamma_{ij}^{\mathrm{dph}}$ is the dominant mechanism in a semiconductor solid state system in contrast to the atomic system.

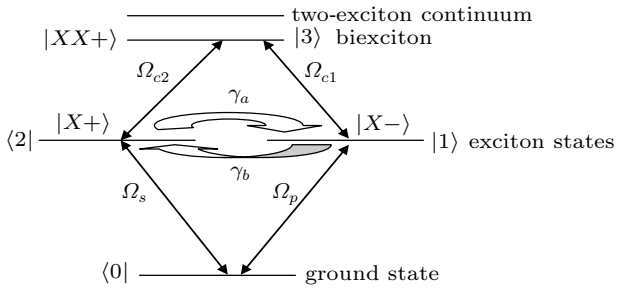


Fig. 1. Energy levels and transitions of the exciton–biexciton states. $|0\rangle$: ground state, $|1\rangle$ and $|2\rangle$: one-exciton states, $|3\rangle$: biexciton state (or two-exciton continuum state).

In the limit of the two-weak probe fields, all excitons will stay in the level $|0\rangle$ and hence we assume that $\rho_{00}=1$. Under this assumption, the steady-state solution of Eq. (1) can be obtained as follows:

$$P_p=\varepsilon_0\chi_pE_p=N\mu_{10}\rho_{10}, \qquad (2)$$

$$P_S=\varepsilon_0\chi_SE_S=N\mu_{20}\rho_{20}. \qquad (3)$$

Therefore, the susceptibilities of the two probe fields can be written as

$$\chi_P=\frac{N|\mu_{10}|^2}{\hbar\varepsilon_0\Omega_P}\rho_{10}=\frac{N|\mu_{10}|^2}{\hbar\varepsilon_0}\chi_P', \qquad (4)$$

$$\chi_S=\frac{N|\mu_{20}|^2}{\hbar\varepsilon_0\Omega_S}\rho_{20}=\frac{N|\mu_{20}|^2}{\hbar\varepsilon_0}\chi_S', \qquad (5)$$

where N is the density of carriers and μ_{10} and μ_{20} are the dipole matrix elements between $|0\rangle$ and $|1\rangle$, $|2\rangle$. Thus, we can obtain

$$\chi_P'=\frac{\Omega_{c2}^2-b_2b_3-\Omega_{c1}\Omega_{c2}\Omega_S\mathrm{e}^{\mathrm{i}\phi}/\Omega_p}{b_1b_2b_3-b_2(\Omega_{c2}^2+\Omega_{c1}^2)}, \qquad (6)$$

$$\chi_S'=\frac{\Omega_{c1}^2-b_2b_3-\Omega_{c1}\Omega_{c2}\Omega_P\mathrm{e}^{-\mathrm{i}\phi}/\Omega_S}{b_1b_2b_3-b_2(\Omega_{c2}^2+\Omega_{c1}^2)}. \qquad (7)$$

Here, $b_1=-(1/2(\gamma_4+\gamma_b+\gamma_{10}^{\mathrm{dph}})-\mathrm{i}\Delta_1)$, $b_2=-(1/2(\gamma_3+\gamma_a+\gamma_{20}^{\mathrm{dph}})-\mathrm{i}\Delta_2)$, and $b_3=-(1/2(\gamma_1+\gamma_2+\gamma_{30}^{\mathrm{dph}})-\mathrm{i}\Delta_3)$.

By this model, we can also determine the light group velocity, according to Ref. [71], as follows:

$$v_{\mathrm{g}}\equiv\frac{\mathrm{d}\omega}{\mathrm{d}k}=\frac{c}{n+\omega(\mathrm{d}n/\mathrm{d}\omega)}, \qquad (8)$$

where $n\simeq 1+2\pi\chi$, and then

$$\frac{c}{v_{\mathrm{g}}}=1+2\pi\mathrm{Re}(\chi(\omega))+2\pi\omega\mathrm{Re}(\mathrm{d}\chi/\mathrm{d}\omega). \qquad (9)$$

It is found that from Eq. (9), when $\mathrm{Re}\chi(\omega)$ is zero and the dispersion is very steep and positive, the group velocity is reduced and then

$$\frac{c}{v_{\mathrm{g}}}-1=2\pi\omega\mathrm{Re}(\mathrm{d}\chi/\mathrm{d}\omega). \qquad (10)$$

3. Results and discussion

Now, based on the various physical parameters of the system, the two-weak probe absorption, dispersion, and group velocity of the incident pulses are displayed. The transient behaviors of the absorption, dispersion, and exciton population at various levels are also discussed. The curves of absorption, dispersion, and group velocity versus probe and signal field detuning for different situations of coupling fields are shown in parts (a) and (b) of Fig. 2. The solid line corresponds to the case $\Omega_{c1} = \Omega_{c2}$, dashed line refers to the case $\Omega_{c1} \ll \Omega_{c2}$ and dotted line denotes the case $\Omega_{c1} \gg \Omega_{c2}$. It can be seen that for $\Omega_{c1} = \Omega_{c2}$ and $\Omega_{c1} \ll \Omega_{c2}$, the probe absorption corresponds to a negative slope dispersion. In this case group velocity has a negative value which corresponds to superluminal light propagation. Also, from the dashed line it can be concluded that the large refractive index corresponds to a high absorptive peak which is called electromagnetically induced absorption (EIA).[72] However, for $\Omega_{c1} \gg \Omega_{c2}$ (dotted line), the absorption spectrum is essentially negative (gain) for a wide range of Δ_p. It is clearly seen that the slope of dispersion becomes positive, corresponding to the subluminal light propagation. The curve of corresponding group velocity versus probe field detuning is also shown. This is in good agreement with previous result. The curves of signal absorption, dispersion, and group velocity versus signal field detuning for different ratios between Rabi frequencies of two control field are shown in part (b) of Fig. 2. By comparing the obtained results with previous results in part (a), it can be seen that the normal dispersion and subluminal light propagation are amplified for $\Omega_{c1} \ll \Omega_{c2}$ (dashed line). However, sharp peak absorption (EIA) with large refractive index and superluminal light propagation occurs for $\Omega_{c1} \gg \Omega_{c2}$ (dotted line). In Fig. 3, for $\Omega_{c1} \gg \Omega_{c2}$, the variations of absorption (a), dispersion (b), and group velocity (c) of the probe field with probe detuning Δ_p for different values of the signal field detuning are displayed. From panel (a) of Fig. 3, it can be seen that the probe amplification occurs for any value of signal field detuning. The behaviors of probe dispersion spectrum versus probe detuning are shown in panel (b) of Fig. 3. In this case, for $\Delta_s = -\Delta_p/2$ the slope of dispersion changes from positive to negative value. The variations of the corresponding group velocity with probe field detuning are also shown in panel (c) of Fig. 3. It can be seen that the switching from subluminal to superluminal light propagation or *vice versa* can be obtained. In Fig. 4, for $\Omega_{c1} \ll \Omega_{c2}$, the properties of absorption (a), dispersion (b), and group velocity (c) of the signal field versus the signal detuning Δ_s for different values of the probe field detuning are displayed. These results are the

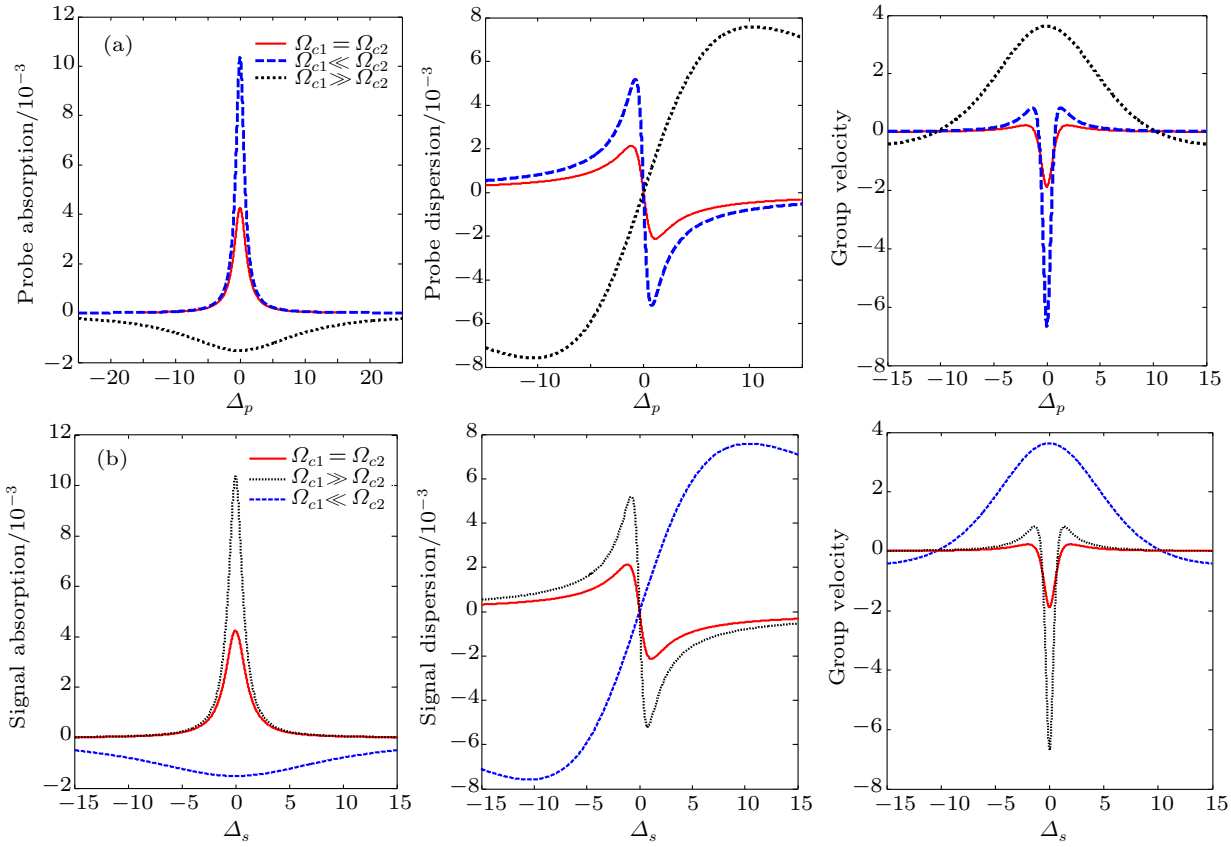


Fig. 2. (color online) Variations of absorption, dispersion, and group velocity with field detuning for probe field (a) and signal field (b). The solid line corresponds to the case $\Omega_{c1} = \Omega_{c2}$, dashed line the case $\Omega_{c1} \ll \Omega_{c2}$, and dotted line the case $\Omega_{c1} \gg \Omega_{c2}$. The selected parameters are $\gamma_1 = \gamma_2 = \gamma_3 = \gamma_4 = 2, \gamma_{ij}^{\rm dph} = 1, \gamma_a = \gamma_b = 0, \phi = 0, \Delta_3 = 0$.

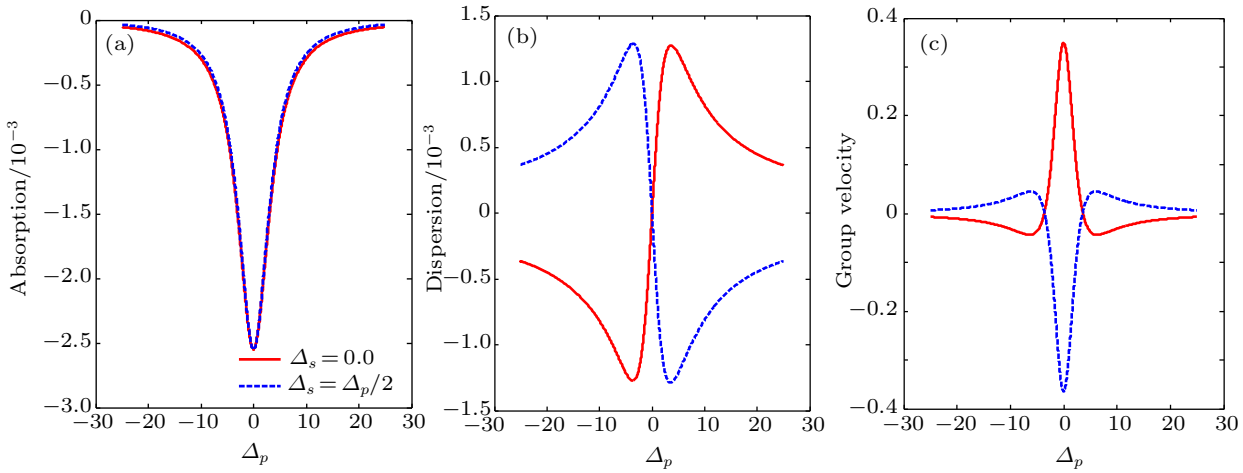


Fig. 3. (color online) Variations of absorption (a), dispersion (b), and group velocity (c) with probe field detuning for $\Omega_{c1} \gg \Omega_{c2}$. The solid line corresponds to the case $\Delta_s = 0$, and dashed line the case $\Delta_s = -\Delta_p/2$. Other parameters are same as those in Fig. 2.

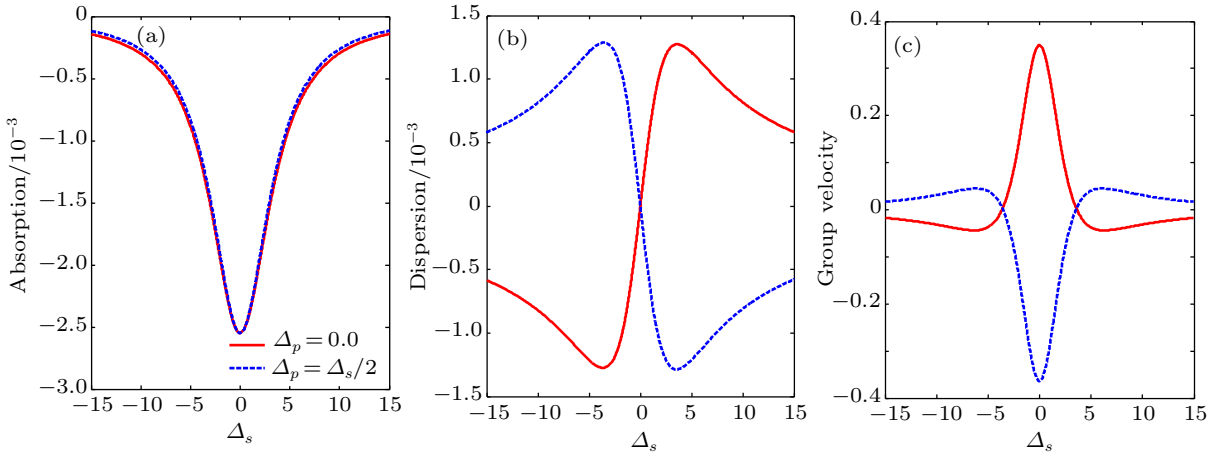


Fig. 4. (color online) Variations of absorption (a), dispersion (b), and group velocity (c) with signal field detuning for $\Omega_{c1} \gg \Omega_{c2}$. The solid line corresponds to $\Delta_p = 0$, and dashed line the $\Delta_p = -\Delta_s/2$. Other parameters are same as those in Fig. 2.

same as those shown in Fig. 3. The effects of relative phase between applied fields on the probe and signal absorption, dispersion, and group velocity are discussed in Fig. 5. It is clearly seen that for $\Omega_{c1} \gg \Omega_{c2}$, by changing the relative phase from 0 to π, the probe amplification is converted into the probe absorption, and the positive slope of dispersion changes into the negative slope of dispersion. In this case, the switching from subluminal to superluminal speed in group velocity of propagated light is present. Here, subluminal light corresponds to probe amplification and superluminal light corresponds to probe absorption. However, in the signal field case, by changing the relative phase from 0 to π, the signal absorption is enhanced which is accompanied with no change in slope of dispersion and with the increase of the value of refractive index as well. Thus a large refractive index corresponds to a high absorptive peak which corresponds to EIA in the medium. Also, the negative value of group velocity is relevant to superluminal light propagation in the medium. As shown in Fig. 6, the behaviors of absorption, dispersion, and group velocity in the case of $\Omega_{c1} \ll \Omega_{c2}$, for the probe field (a) and signal field (b) are analyzed. In Fig. 8(a), it can be seen that the absorption, dispersion, and group velocity all seem to be periodic. Furthermore, a large index of refraction with high absorption peak and superluminal light propagation is observed. Figure 8(b) shows the absorption, dispersion, and group velocity of the signal field in the case of $\Omega_{c1} \ll \Omega_{c2}$. From absorption spectrum it can be seen that the amplification can be achieved for a large range of phase ϕ. By the consideration of dispersion spectrum, it is found that a large refractive index of refraction with zero absorption can be obtained by changing the relative phase. It is well known that for optical communication a large index of refraction with zero absorption is useful and applicable. Furthermore, by changing the relative phase between applied fields, the switching between subluminal light propagation and superluminal light propagation occurs. In this case, subluminal light propagation corresponds to signal amplification and superluminal light propagation corresponds to a weak absorption. Comparing Fig. 6(a) for the probe field with

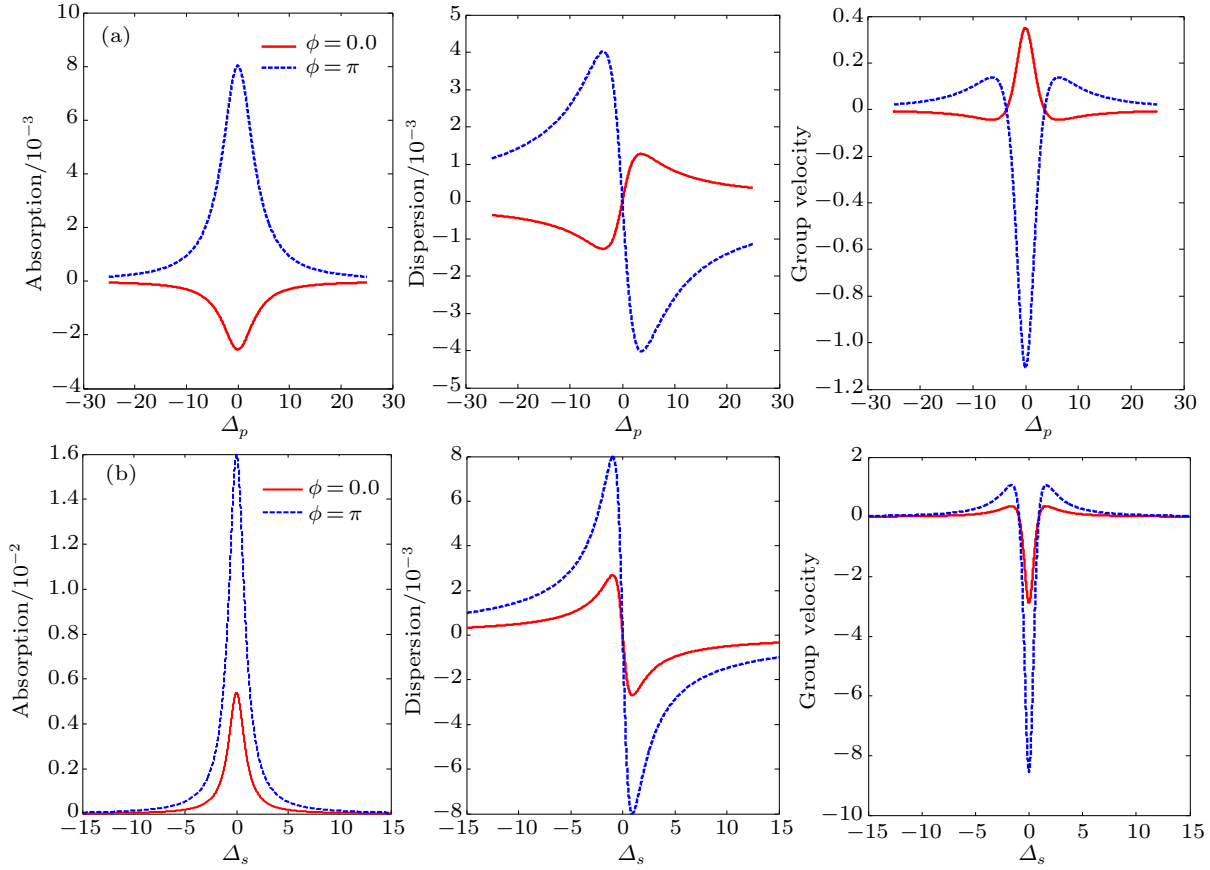


Fig. 5. (color online) Variations of absorption, dispersion, and group velocity with field detuning for probe field (a) and signal field (b) in the case $\Omega_{c1} \gg \Omega_{c2}$. The solid line corresponds to the case $\phi = 0$, and dashed line the case $\phi = \pi$. Other parameters are same as those in Fig. 2.

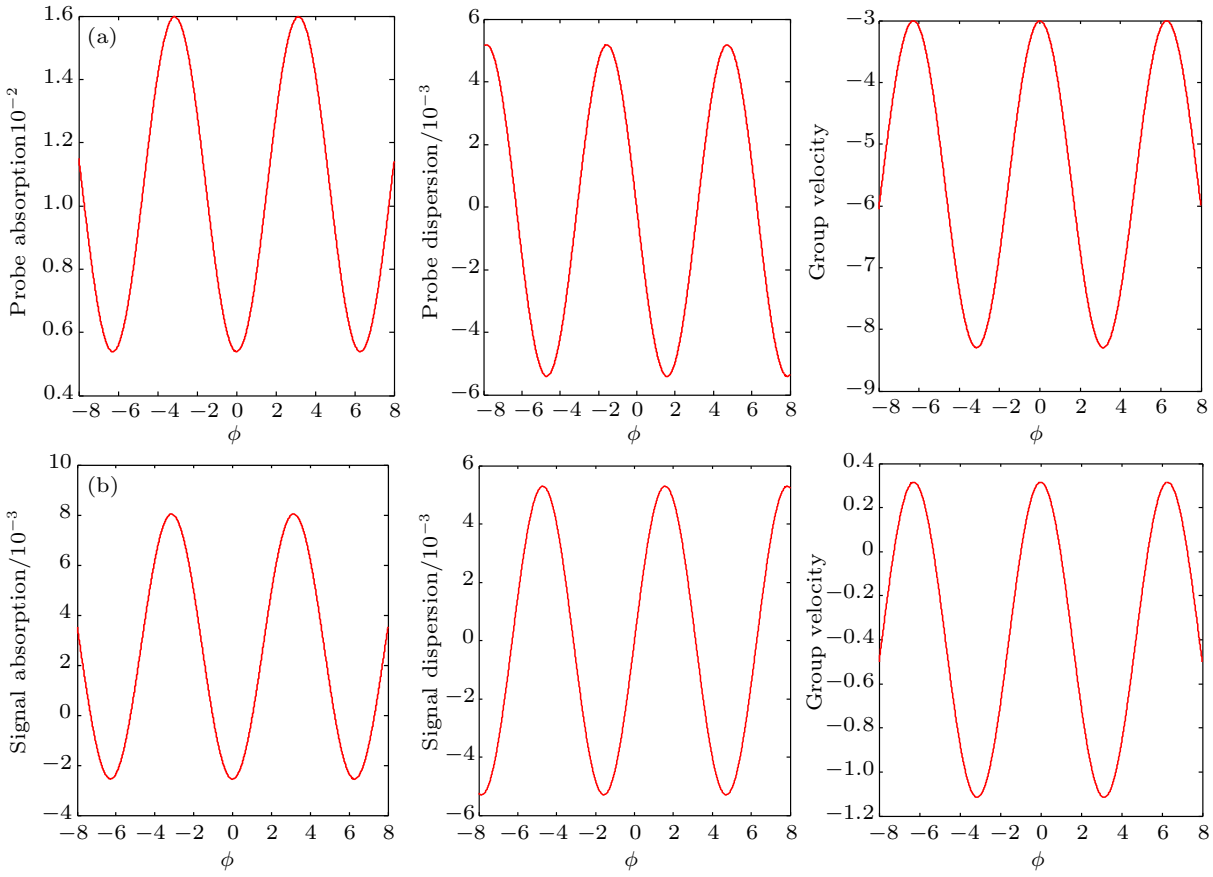


Fig. 6. (color online) Variations of absorption, dispersion, and the group velocity with relative phase for probe field (a) and signal field (b) in the case $\Omega_{c1} \ll \Omega_{c2}$. The selected parameters are same as those in Fig. 2.

Fig. 6(b) for the signal field, it can be seen that for the probe field, a large index of refraction corresponds to a high absorption, and for signal field a large index of refraction with zero absorption is located at different values of the relative phase. Shown in Fig. 7(a) is the transient behavior of the absorption–dispersion for probe field. For the weak probe field, when we set $\Omega_{c1} = \Omega_{c2}$ (solid line), the absorption is equal to zero and starts to increase as the time increases, and finally reaches a steady state value. By increasing the Rabi frequency Ω_{c2} and for $\Omega_{c1} \ll \Omega_{c2}$ (dashed line), the absorption is enhanced as the time increases and finally reaches a large absorption at a steady state. For $\Omega_{c1} \gg \Omega_{c2}$ (dotted line), the probe absorption changes to probe gain. The corresponding dispersions for different Rabi-frequencies for coupling fields are also plotted. It is found that for $\Omega_{c1} = \Omega_{c2}$ (solid line), the dispersion is negative and the light pulse is accompanied with absorption. By increasing the Rabi frequency Ω_{c2} and for $\Omega_{c1} \ll \Omega_{c2}$ (dashed line), the negative value of dispersion is enhanced. However, for $\Omega_{c1} \gg \Omega_{c2}$ (dotted line), the dispersion changes from negative to positive value and the light pulse is accompanied with negative absorption (gain). The transient behavior of the absorption–dispersion for signal field is shown in Fig. 7(b). It can be seen that for $\Omega_{c1} = \Omega_{c2}$ (solid line), the similar results to those shown in Fig. 7(a) are obtained. But for $\Omega_{c1} \ll \Omega_{c2}$ (dashed line) and $\Omega_{c1} \gg \Omega_{c2}$ (dotted line), the obtained results are opposite to those shown in Fig. 7(a). The effects of exciton spin relaxation on transient behaviors of absorption and dispersion for probe field are displayed in Fig. 8(a). It is found that by enhancing the exciton spin relaxation between exciton levels, the probe gain decreases, but increases in the medium. Moreover, the dispersion values of the probe light are negative for the different values of the exciton spin relaxation. In Fig. 8(b), the effect of exciton spin relaxation on transient behavior of the signal field is discussed. It can be seen that by enhancing the exciton spin relaxation the signal absorption reduces its minimum value. However, the dispersion value of the signal is also negative. Thus the superluminal light propagation can be obtained in the weak signal absorption. The transient behaviors of the absorption and dispersion of the probe field for the various values of the relative phase are shown in Fig. 9(a). For $\phi = 0$, at time $t = 0$ the absorption is a positive value; as time increases, it starts to oscillate and finally reaches a negative steady state value. In this case, at time $t = 0$, the absorption is zero; as time increases, it starts to oscillate and finally reaches a positive steady state, so subluminal group velocity is accompanied with amplification. For $\phi = \pi/2$ and $\phi = \pi$, the absorption becomes positive and dispersion becomes negative, so superluminal light is accompanied with an absorption. However, for $\phi = \pi/2$, the values of absorption is less than $\phi = \pi$. In Fig. 9(b), the effect of relative phase on transient behavior of the signal field is discussed.

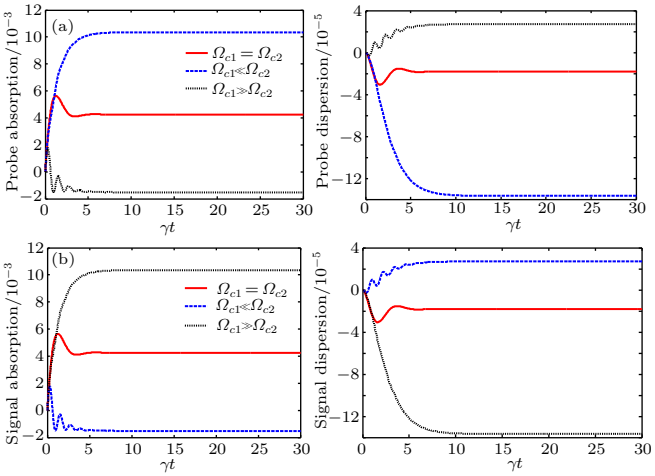


Fig. 7. (color online) Time evolutions of the absorption, dispersion for probe field (a) and signal field (b). The solid line corresponds to the case $\Omega_{c1} = \Omega_{c2}$, dashed line the case $\Omega_{c1} \ll \Omega_{c2}$ and dotted line the case $\Omega_{c1} \gg \Omega_{c2}$. The selected parameters are same as those in Fig. 2.

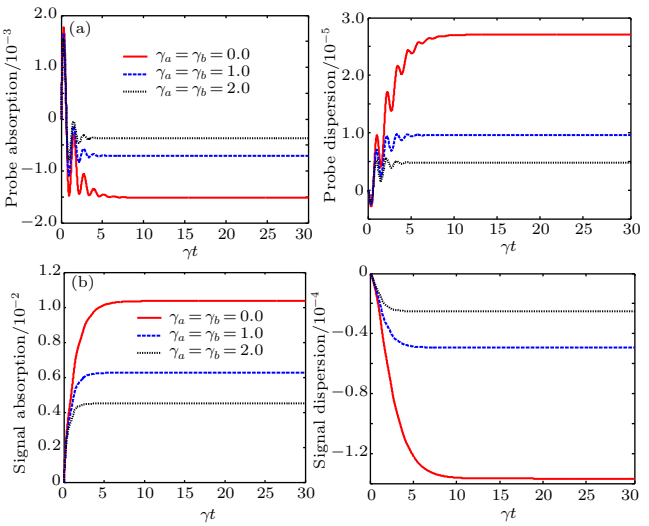


Fig. 8. (color online) Time evolutions of the absorption, dispersion for probe field (a) and signal field (b) for the case $\Omega_{c1} \gg \Omega_{c2}$. The solid line corresponds to $\gamma_a = \gamma_b = 0$, dashed line the case $\gamma_a = \gamma_b = 1$, and dotted line the case $\gamma_a = \gamma_b = 2$. The selected parameters are same as those in Fig. 2.

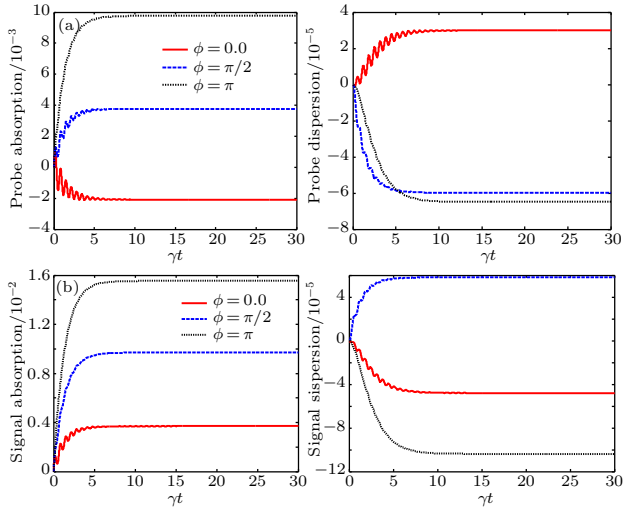


Fig. 9. (color online) Time evolutions of absorption and dispersion for probe field (a) and signal field (b) for the case $\Omega_{c1} \approx \Omega_{c2}$. The solid line corresponds to the case $\phi = 0$, dashed line the case $\phi = \pi/2$, and dotted line the case $\phi = \pi$. The selected parameters are same as those in Fig. 2.

It can be seen that for $\phi = 0$, at time $t = 0$, the absorption and dispersion are zero; As time increases, they start to oscillate and finally reach a steady state value. The steady state value is positive for signal absorption and is negative for dispersion. Thus, the superluminal light is corresponding to a little absorption. By changing the relative phase from $\phi = 0$ to $\phi = \pi/2$, the absorption increases and negative dispersion changes into positive dispersion. Thus subluminal light is corresponding to the high absorption. By enhancing the relative phase to $\phi = \pi$, the dispersion becomes negative and the value of absorption also increases. The transient behaviors of population inversion between different levels for different ratios of Rabi frequencies are displayed in Fig. 10. It can be seen that for $\Omega_{c1} = \Omega_{c2}$ (a), the population inversion between different levels cannot occur. However, for $\Omega_{c2} \gg \Omega_{c1}$ (b), and $\Omega_{c1} \gg \Omega_{c2}$ (c) population inversions between levels $|3\rangle$, $|2\rangle$ and $|3\rangle$, $|1\rangle$ occur respectively, and those between other levels cannot occur. Physically, when $\Omega_{c2} \gg \Omega_{c1}$ or $\Omega_{c1} \gg \Omega_{c2}$, most excitons transfer between levels $|3\rangle$, $|2\rangle$ and $|3\rangle$, $|1\rangle$, thus most excitons are trapped in level $|3\rangle$.

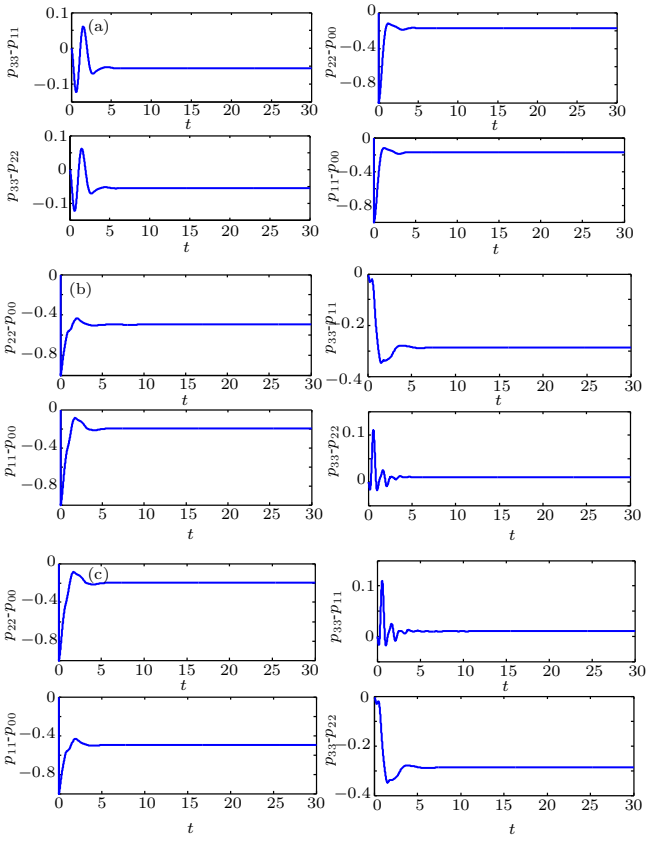


Fig. 10. (color online) Time evolutions of population inversion for the cases: $\Omega_{c1} = \Omega_{c2}$ (a), $\Omega_{c1} \ll \Omega_{c2}$ (b), and $\Omega_{c1} \gg \Omega_{c2}$ (c). The selected parameters are same as those in Fig. 2.

4. Conclusion

In this paper, the transient and steady-state optical properties of two weak probe light beams in an exciton–biexciton system are studied. The results show that amplifications, dispersions, and group indexes of the probe and signal fields can be adjusted by the relative phase between applied fields and the intensity of the coupling field. It is also shown that the exciton spin relaxation can affect the transient behavior of the medium. Our proposed model with flexible design and widely adjustable parameters can provide a new possibility of technological applications in the light amplification and light propagation between subluminal and superluminal speed in the solid-state materials.

References

[1] Chow W W, Schneider H C and Phillips M C 2003 *Phys. Rev. A* **68** 053802
[2] Ma S M, Xu H and Ham B S 2009 *Opt. Express* **17** 148902
[3] Philips M and Wang H L 2004 *Phys. Rev. B* **69** 115337
[4] Phillips M C and Wang H L 2002 *Phys. Rev. Lett.* **89** 186401
[5] Wu Y and Yang X 2005 *Phys. Rev. A* **71** 053806
[6] Silvestri L, Bassani F and Czajkowski G 2002 *Physica Status Solidi* **190** 683
[7] Frogley M D, Dynes J F and Beck M 2006 *Nat. Matter* **5** 175
[8] Wu Y, Saldana J and Zhu Y 2003 *Phys. Rev. A* **67** 013811
[9] Wu Y and Yang X 2004 *Phys. Rev. A* **70** 053818
[10] Wu Y 2008 *J. Appl. Phys.* **103** 104903
[11] Wu Y and Yang X 2007 *Phys. Rev. B* **76** 054425
[12] Li J H 2007 *Phys. Rev. B* **75** 155329
[13] Li J H 2007 *Opt. Commun.* **274** 366
[14] Li J H, Hao X, Liu J and Yang X 2008 *Phys. Lett. A* **372** 716
[15] Li J H and Hao X Y 2008 *Mod. Phys. Lett. B* **22** 393
[16] Li J H and Yang X X 2006 *Eur. Phys. J. B* **53** 449
[17] Wang Z and Xu M 2009 *Opt. Commun.* **282** 1574
[18] Wang Z 2009 *Opt. Commun.* **282** 4745
[19] Wang Z, Yu B, Zhen S, Wu X, Zhu J and Cao Z 2012 *Superlattices and Microstructure* **51** 324
[20] Wang Z 2011 *J. Lumin.* **131** 2404
[21] Asadpour S H, Jaberi M and Rahimpour Soleimani H 2013 *J. Opt. Soc. Am. B* **30** 1815
[22] Naseri T, Asadpour S H and Sadighi-Bonabi R 2013 *J. Opt. Soc. Am. B* **30** 641
[23] Asadpour S H and Eslami-Majd A 2012 *J. Lumin.* **132** 1477
[24] Asadpour S H and Hamedi H R 2013 *Opt. Quantum Electron.* **45** 11
[25] Ai J F, Chen A X and Deng Li 2013 *Chin. Phys. B* **22** 024209
[26] Joshi A and Xiao M 2004 *Appl. Phys. B: Lasers Opt.* **79** 65
[27] Zhang D, Yu R, Li J H, Ding C and Yang X 2013 *Phys. Lett. A* **377** 2621
[28] Liu S, Li J, Yu R and Wu Y 2013 *Phys. Rev. A* **87** 062316
[29] Liu S, Li J, Yu R and Wu Y 2013 *Phys. Rev. A* **87** 042306
[30] Li J H, Yu R and Wu Y 2013 *J. Appl. Phys.* **113** 103104
[31] Liu S, Li J, Yu R and Wu Y 2013 *Opt. Express* **21** 3501
[32] Xiong H, Si L G, Lu X Y, Yang X and Wu Y 2013 *Opt. Lett.* **38** 353
[33] Wu Y and Yang X 2007 *Appl. Phys. Lett.* **91** 094104
[34] Hao X, Si L G, Ding C, Huang P, Li J and Yang X 2010 *J. Opt. Soc. Am. B* **27** 1792
[35] Si L G, Yang W X, Lü X Y, Hao X and Yang X 2010 *Phys. Rev. A* **82** 013836
[36] Osman K I and Abd-Elnabi S 2014 *J. Lumin.* **147** 346
[37] Li J, Yu R, Si L G and Yang X 2010 *J. Phys. B: At. Mol. Opt. Phys.* **43** 065502
[38] Osman K I, Hassan S S and Joshi A 2009 *Eur. Phys. J. D* **54** 119
[39] Osman K I and Joshi A 2012 *Phys. Lett. A* **376** 2565
[40] Osman K I and Joshi A 2012 *Opt. Commun.* **293** 86
[41] Asadpour S H and Rahimpour Soleimani H 2014 *Physica B* **434** 112
[42] Asadpour S H and Golsanamlou Z and Rahimpour Soleimani 2013 *Physica E* **54** 45
[43] Asadpour S H and Rahimpour Soleimani H 2014 *Opt. Commun.* **315** 394
[44] Asadpour S H and Rahimpour Soleimani H 2013 *Superlattices and Microstructure* **62** 217
[45] Asadpour S H, Sahrai M, Soltani A and Hamedi H R 2012 *Phys. Lett. A* **376** 147

[46] Harris S E 1997 *Phys. Today* **50** 36
[47] Hau L V, Harris S E, Datton Z and Behroozi C H 1999 *Nature* **397** 594
[48] Kash M M, Sautenkov V A, Zibrov A S, Hollberg L, Welch G R, Lukin M D, Rostovtsev Y, Fry F S and Scully M O 1999 *Phys. Rev. Lett.* **82** 5229
[49] Scully M O and Zubairry M S 1997 *Quantum Optics* (London: Cambridge University Press) p. 225
[50] Chemla S and Shah J 2001 *Nature* **411** 549
[51] Serapiglia G B, Paspalakis E, Sirtori C, Vodopyanov K L and Philips C C 2000 *Phys. Rev. Lett.* **84** 1019
[52] Dynes J F, Frogley M D, Rodger J and Philips C C 2005 *Phys. Rev. B* **72** 085323
[53] Dynes J F, Frogley M D, Beck M, Faist J and Philips C C 2005 *Phys. Rev. Lett.* **94** 157404
[54] Philips M and Wang H 2003 *Opt. Lett.* **28** 831
[55] Philips M and Wang H 2003 *Phys. Rev. Lett.* **90** 183602
[56] Yang W X, Chen A X, Lee R K and Wu Y 2011 *Phys. Rev. A* **84** 013835
[57] Yan W, Wang T and Li X M 2012 *Opt. Commun.* **285** 3559
[58] Lindberg L and Binder M R 1995 *Phys. Rev. Lett.* **75** 1403
[59] Fleischhauer M, Imamoglu A and Marangos J P 2005 *Rev. Mod. Phys.* **77** 633
[60] Liu C, Dutton Z, Behroozi C H and Hau L V 2001 *Nature* **409** 490
[61] Voss T, Ruckmann I and Gutowski J 2006 *Phys. Rev. B* **73** 115311
[62] Wang L G, Qamar S and Zhu S Y 2008 *Phys. Rev. A* **77** 033833
[63] Hao X Y, Ding C L and Lu X Y 2010 *Physica E* **42** 1984
[64] Sun H, Niu Y P and Jin S Q 2007 *J. Phys. B: At. Mol. Opt. Phys.* **40** 3037
[65] Peng Y G and Zheng Y J 2008 *Appl. Phys. Lett.* **92** 092120
[66] Wang D S and Zheng Y J 2011 *Phys. Rev. A* **83** 013810
[67] Kang H S, Hernandez G and Zhang J P 2006 *Phys. Rev. A* **73** 011802
[68] Yan W, Wang T and Li X M 2012 *Opt. Commun.* **285** 3559
[69] Yan W, Wang T, Li X M and Jin Y J 2012 *J. Mod. Opt.* **59** 784
[70] Yan W, Wang T, Li X M, Dong C, Yu C and Tang J 2013 *Phys. Status Solidi B* **250** 1384
[71] Boyd R W and Gauthier D J 2002 *Prog. Opt.* **43** 497
[72] Hu X M, Cheng G L, Zou J H, Li X and Du D 2005 *Phys. Rev. A* **72** 023803